

## Article

# Investigation into the Flexural Toughness and Methods of Evaluating Ductile Concrete

Yonggang Ding <sup>1,2</sup>, Yunfei Li <sup>1</sup>, Xiangyang Zhao <sup>1</sup>, Jie Dai <sup>1,2,\*</sup> and Hualong Xu <sup>3</sup><sup>1</sup> College of Civil Engineering, Henan University of Technology, Zhengzhou 450001, China<sup>2</sup> Henan Key Laboratory of Grain and Oil Storage Facility & Safety, HAUT, Zhengzhou 450001, China<sup>3</sup> Banqiao Reservoir Administration, Zhumadian 463000, China

\* Correspondence: daijie@haut.edu.cn; Tel.: +86-186-2371-5769

**Abstract:** The main purpose of this study was to investigate the flexural behavior of high-ductility fiber-reinforced concrete (HDC) and propose a suitable method for evaluating flexural toughness. The flexural strength, deformation, and toughness of HDC were investigated through four-point bending tests with specimens of 40 × 40 × 160 mm. The test parameters were fiber volume fractions (0%, 1%, 1.5%, and 2%), water–binder ratios (0.24, 0.26, 0.29, and 0.32), and ages (28 d and 56 d). The experimental results showed that polyvinyl alcohol (PVA) fibers led to significant improvement in the flexural behavior of HDC due to its strain-hardening behavior and excellent crack dispersion capacity. The ultimate flexural strength of HDC with 2% PVA fibers of about 15.32 MPa showed an increase of up to 221%. The deformation and flexural toughness ratios were 23 times and 1.43 times higher, respectively, than the specimens without fibers. A simple and practical method for evaluating the flexural toughness of HDC was proposed, which solved many problems with the existing methods. This method made full use of the peak load, which overcame the difficulty of identifying the initial crack information, solved the insufficient deflection limit, and provided a more comprehensive and accurate evaluation by selecting characteristic points evenly distributed throughout the loading process.



**Citation:** Ding, Y.; Li, Y.; Zhao, X.; Dai, J.; Xu, H. Investigation into the Flexural Toughness and Methods of Evaluating Ductile Concrete. *Appl. Sci.* **2022**, *12*, 12313. <https://doi.org/10.3390/app122312313>

Academic Editor: Chao-Wei Tang

Received: 11 November 2022

Accepted: 28 November 2022

Published: 1 December 2022

**Publisher's Note:** MDPI stays neutral with regard to jurisdictional claims in published maps and institutional affiliations.



**Copyright:** © 2022 by the authors. Licensee MDPI, Basel, Switzerland. This article is an open access article distributed under the terms and conditions of the Creative Commons Attribution (CC BY) license (<https://creativecommons.org/licenses/by/4.0/>).

**Keywords:** high-ductility fiber-reinforced concrete; flexural behavior; toughness; evaluation method

## 1. Introduction

Concrete is one of the most widely used construction and building materials due to its low cost, high strength, and versatility [1,2]. However, the poor tensile behavior, brittle failure mode, and low deformability of concrete limit its application in civil engineering [3,4]. One way to overcome these drawbacks is to add different fibers, such as steel, polyvinyl alcohol, and polypropylene fibers, to obtain higher tensile strength, better flexural toughness, and excellent seismic performance [5–8]. Nowadays, FRC is used in a variety of applications such as new civil structures, the repair and retrofit of building structures, and underground structures to improve fatigue resistance and seismic performance [9–11].

Flexural toughness fundamentally reflects the toughening effects of fibers and the inner structural performance of matrices; reinforced concrete structures are designed through their application. Many researchers have focused on the flexural behavior and toughness properties of FRC. Tayfun found that the flexural strength of steel fiber-reinforced concrete increased with concrete age and fiber volume fraction, but the first crack development significantly decreased by increasing the fiber volume fraction [12]. Gao et al. investigated the influence of fiber volume content and concrete strength on the flexural behavior of steel fiber-reinforced concrete and observed that the fiber volume content significantly affected the initial and residual flexural toughness ratio of the specimens [13]. Felekoğlu et al. presented that a high-strength matrix with a high-strength fiber gave the best performance from the viewpoint of flexural and toughness performance according to a three-point flexural loading test [14]. The test results showed that using straight steel and micropolyvinyl

alcohol fibers produced composites demonstrating stable deflection–hardening with a multiple cracking phenomenon [15]. Ding et al. reported that a hybrid fiber-reinforced concrete showed significant improvements in the flexural toughness of the concrete and correlated the fractured surface roughness with the flexural toughness of the concrete by topographical analysis [16]. Previous research has shown that the addition of fibers improves post-cracking behavior, reduces the opening of cracks, and counteracts their propagation, as well as increases the toughness of concrete owing to their deboning and pull-out failure mechanisms [15,17]. The specimen response in a bending test was also consistent with the tensile properties of a strain hardening response material, and an inverse analysis was discussed by López et al. [18–21].

However, there is no consistent and recognized flexural toughness evaluation method for FRC, especially for special FRC that exhibits strain hardening behavior under tension, high toughness under compression, and is flexural, which are termed engineered cementitious composites (ECCs) [22–24], high-performance fiber-reinforced cementitious composites (HPFRCCs) [25,26], strain hardening cementitious composites (SHCCs) [27,28], and high ductile fiber-reinforced concrete (HDC) [29–32]. Li et al. pointed out that the ASTM C-1018 method is not appropriate for evaluating the toughness of ultra-high toughness cementitious composites, and modified JSCE-SF4 by expanding its range of deflection limit [33]. Skazlić et al. recommended additional toughness parameters for the evaluation of toughness results obtained by ASTM C-1609 [34]. Li et al. evaluated the flexural toughness of steel fiber-reinforced lightweight aggregate concrete by using ASTM C-1018, ASTM C-1609, JSCE-SF4, and JG/T 472-2015 methods. They considered that the JG/T 472-2015 method could reveal the influence of the fiber in terms of the pre-peak and post-peak behavior [35]. In other cases, the evaluation methods mentioned above were directly used or slightly modified to estimate the toughness of FRC; therefore, the shortcomings of the existing methods have not been conquered.

To evaluate the toughness of strain hardening materials and solve the problems of existing methods, a series of four-point bending tests was designed, and a simple and practical method for evaluating the flexural toughness of HDC was proposed. The influence of the fiber volume content, water–binder ratio, and age on the failure mode, load–deflection curve, flexural strength, and toughness of HDC was also highlighted.

## 2. Experimental Program

### 2.1. Materials

The high ductility concrete used in this study was PO 42.5R ordinary Portland cement produced by Xi'an Yaobai Cement Company in Shaanxi, China, with a specific surface area of 350 m<sup>2</sup>/kg. The fly ash was grade I fly ash provided by a power plant in Henan. Medium and coarse river sand with a fineness modulus of 2.83 was used, and the additive used a polycarboxylic acid superplasticizer produced by the Ruikeda Company in Shaanxi, China. The water reduction rate (mass fraction) was 20–40%. As shown in Figure 1, the short PVA fibers had a length of 12 mm, a diameter of 39 μm, a tensile strength of 1600 MPa, and an elastic modulus of 40 GPa. The properties of the PVA fibers are shown in Table 1.



**Figure 1.** Short polyvinyl alcohol (PVA) fiber.

**Table 1.** Properties of the PVA fibers.

Fiber Type	Length (mm)	Diameter (μm)	Aspect Ratio	Tensile Strength (MPa)	Elastic Modulus (GPa)
PVA	12	39	310	1600	40

2.2. *Mixing and Casting*

The target cubic compressive strength of the concrete was 50 MPa. Three test pieces were made for each mixture. The binding material was composed of cement and fly ash with a mass ratio of 1:1. The contrast mixture proportion had a fiber content of 0%, a water–binder ratio (mass ratio) of 0.29, and a sand–binder ratio of 0.36. To examine the influence of the age, water–binder ratio, and fiber–volume fraction on the flexural toughness and properties of HDC, 10 group specimens were made, as shown in Table 2. In the specimen ID, the number after the HC is the age, and the subsequent data represent the fiber content and the water-to-gel ratio. For example, HC56-1-29 means that the sample age was 56 d, the fiber volume content was 1%, and the water–binder ratio was 0.29. The mixing procedure is shown in Figure 2.

**Table 2.** Mixture proportions of HDC.

Group	Specimen ID	Binding Material		Water	Sand	Fiber Volume Fraction (%)
		Cement	Fly Ash			
Control	HC56-0-29	0.5	0.5	0.29	0.36	0
Series I	HC56-1-29	0.5	0.5	0.29	0.36	1.0
	HC56-1.5-29	0.5	0.5	0.29	0.36	1.5
	HC56-2-29	0.5	0.5	0.29	0.36	2.0
	HC56-2-26	0.5	0.5	0.26	0.36	2.0
	HC56-2-32	0.5	0.5	0.32	0.36	2.0
Series II	HC28-1-29	0.5	0.5	0.29	0.36	1.0
	HC28-1.5-29	0.5	0.5	0.29	0.36	1.5
	HC28-2-29	0.5	0.5	0.29	0.36	2.0
	HC28-2-24	0.5	0.5	0.24	0.36	2.0
	HC28-2-26	0.5	0.5	0.26	0.36	2.0

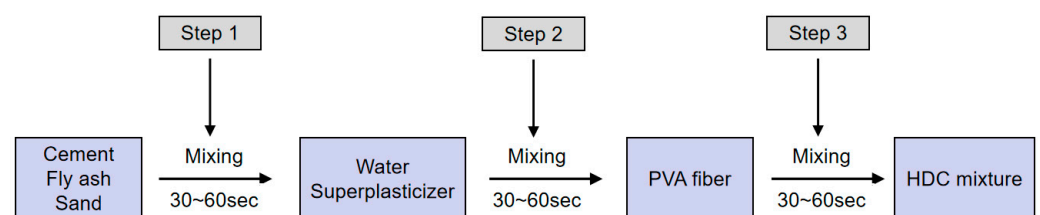


**Figure 2.** HDC mixing process flowchart.

2.3. *Four-Point Flexural Test*

In this study, a beam specimen with a size of 40 mm × 40 mm × 160 mm was used for experimental research on the bending behavior of high-ductility fiber-reinforced concrete. The loading method was four-point loading, as shown in Figure 3. The loading rate was 0.18 mm/min, and the full load-deflection curve of the specimen was collected during loading and used for the bending toughness analysis. The loading device is shown in Figure 3.

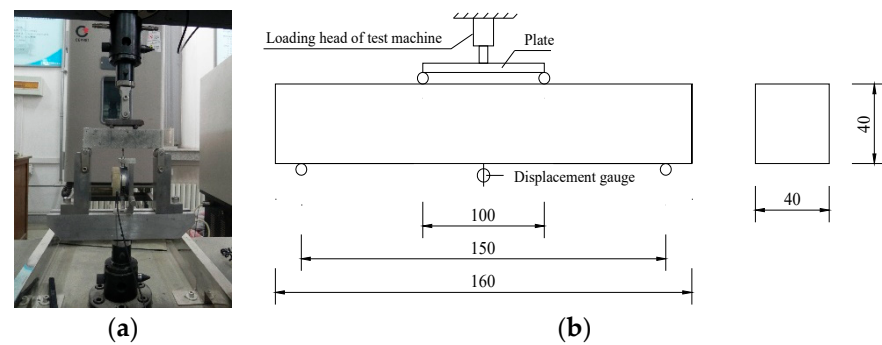


**Figure 3.** Four-point flexural testing apparatus: (a) test apparatus; (b) loading diagram.

### 3. Test Results

#### 3.1. Test Piece Failure Process

When the fiber content was 0%, the plain concrete specimens had brittle fractures along the initial cracks when they were loaded to the peak load (Figure 4). For the HDC beam, the deformation was very large and many fine cracks appeared, but the integrity was always maintained, indicating that the crack-break nature of the plain concrete specimen was essentially changed by the fiber addition (Figure 5). It could be concluded that HDC could not only improve the bearing capacity and deformation ability before failure, but could also make the failure clearly predictable, which is of great significance for engineering safety [36–38].



**Figure 4.** Failure pattern of the control specimens.

With the increase in fiber content, the number of cracks in the HDC test specimens significantly increased, but the width of the cracks gradually decreased. As the PVA fibers spanned the cracks, thus preventing the cracks from developing or reaching a stable state, stress redistribution occurred in the bending and tensile zone, which caused new cracks in the test specimens at other weak areas. As a result, the gap between the cracks decreased with an increase in fiber content.

Compared with the specimens at 56 d of age, the cracks of the HDC beams at 28 d of age were finer and more evenly distributed. Due to a large amount of fly ash in the test specimen, the early hydration rate was slow. Meanwhile, the compressive strength was lower and the bonding strength between fibers and cement was weaker for HDC beams at 28 d. Therefore, the fiber could more easily pull out and would extend more energy in the process, which would increase the pseudo-strain hardening effect of HDC.

#### 3.2. Load-Deflection Curve

The load-deflection curve of the plain concrete specimen was linear. After reaching the peak load, it dropped to zero and the specimen suddenly broke down, as shown in Figure 6a. With an increase in the fiber content, the load-deflection curve of HDC (which was especially fuller in the rising section), the peak load, and its corresponding deflection also continued to increase, showing good toughness performance (Figure 6b–k).

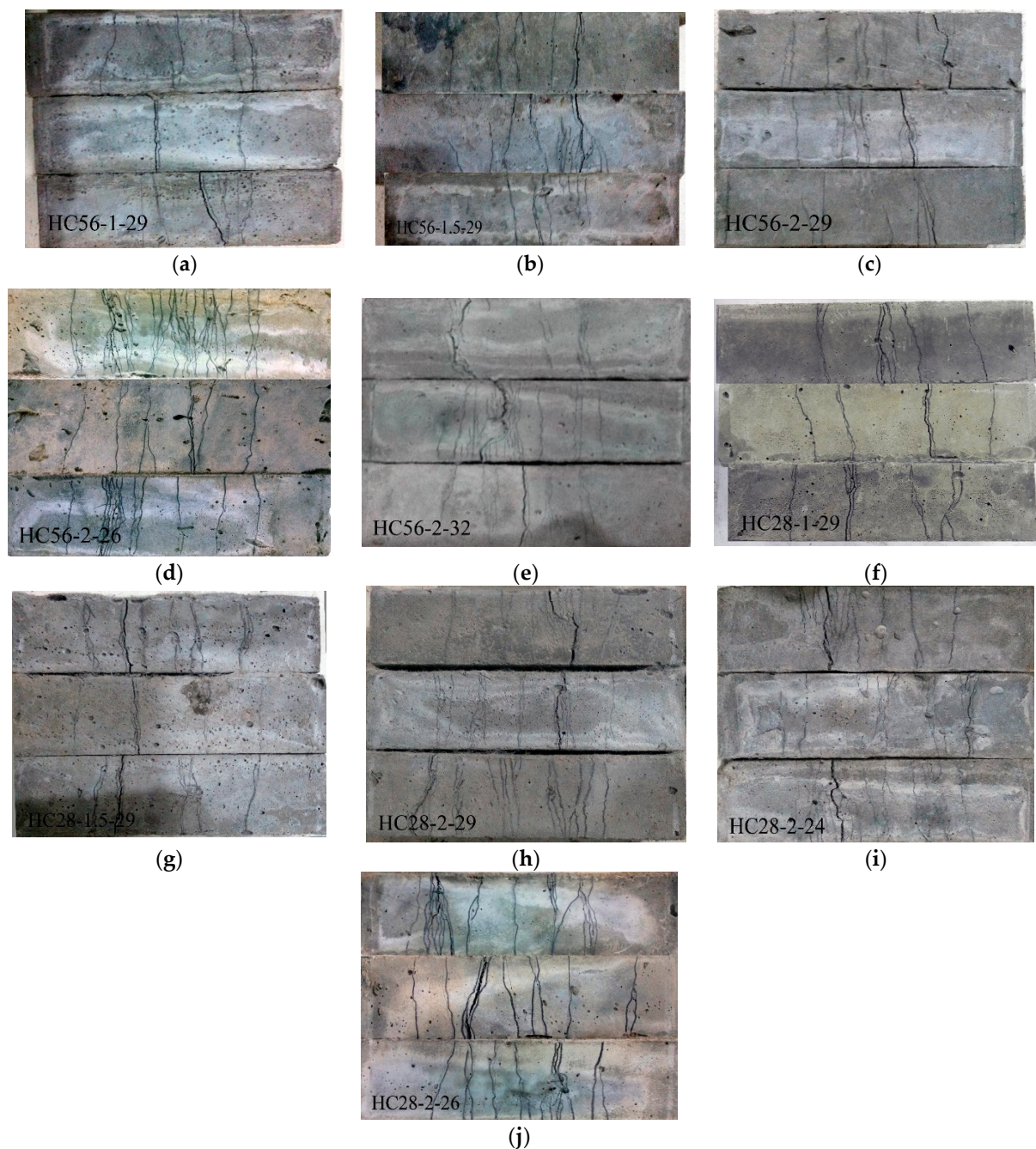


**Figure 5.** Failure pattern of the HDC specimens: (a) HC56-1-29; (b) HC56-1.5-29; (c) HC56-2-29; (d) HC56-2-26; (e) HC56-2-32; (f) HC28-1-29; (g) HC28-1.5-29; (h) HC28-2-29; (i) HC28-2-24; (j) HC28-2-26.

### 3.3. Discussion

The flexural strength and deflection parameters corresponding to the peak load of each group are shown in Table 3. It can be seen that the bending strength and deformation of HDC increased relative to the reference specimen. When the fiber content was 1%, 1.5%, and 2%, the increase in HDC flexural strength  $f_{\max}$  was 59%, 149%, and 221%, respectively. The deflection corresponding to the peak load could reach 10~20 times that of the plain concrete test piece. As seen in Figure 7, the effect of increasing the deformation capacity of HDC by increasing the number of fibers was better than the improvement in its bending strength. This was because the fibers at the cracks were gradually pulled out or broken after the specimen cracked, continuously absorbing energy, and its deformation ability was significantly enhanced.

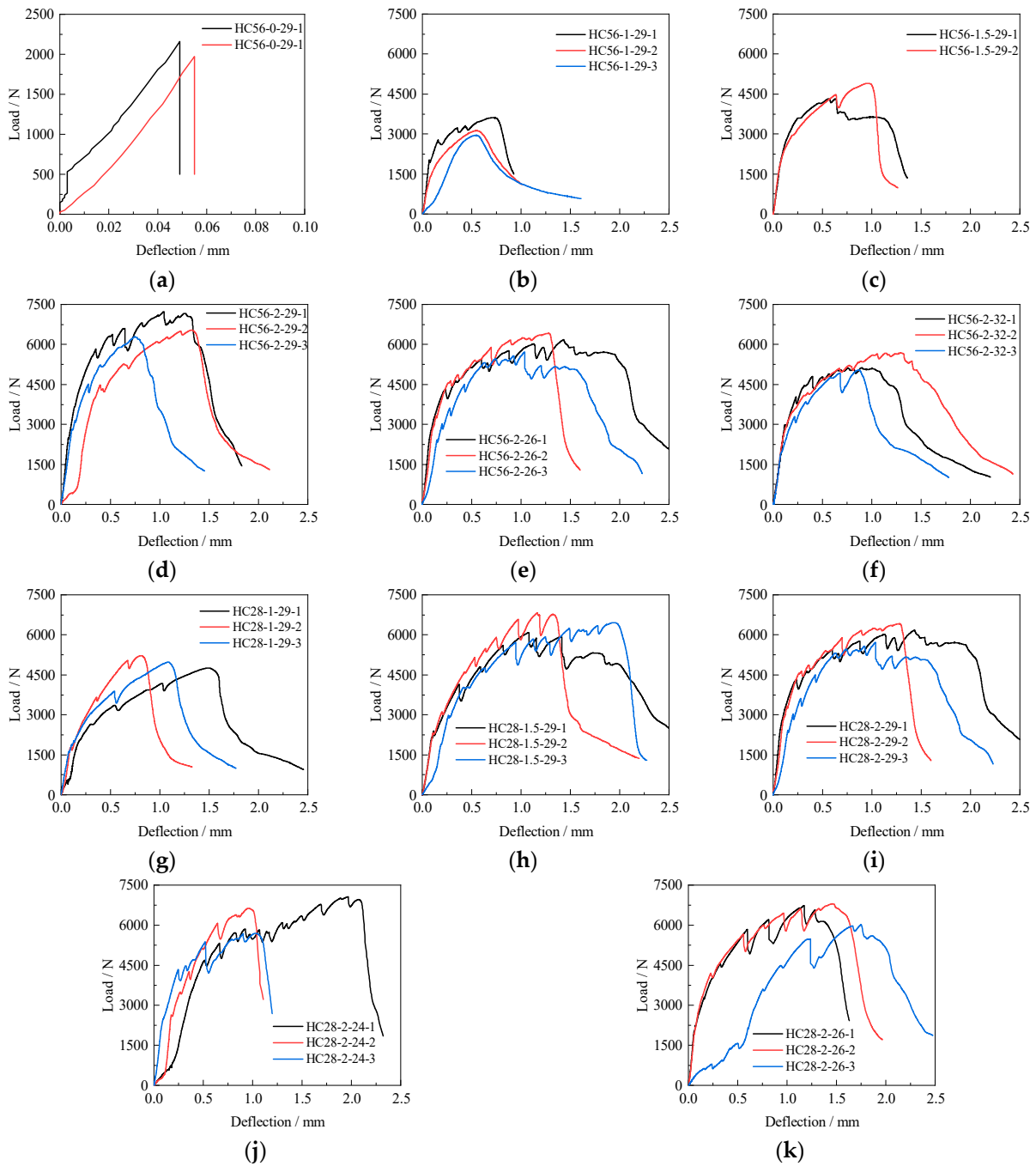


**Figure 6.** Load-deflection curves: (a) HC56-0-29; (b) HC56-1-29; (c) HC56-1.5-29; (d) HC56-2-29; (e) HC56-2-26; (f) HC56-2-32; (g) HC28-1-29; (h) HC28-1.5-29; (i) HC28-2-29; (j) HC28-2-24; (k) HC28-2-26.

It can be seen from Figure 8 that with an increase in the water–binder ratio, the energy dissipation capacity of the HDC beam gradually increased, and the corresponding deflection range of its bending strength and peak load was about 10%. This was because the higher the water-to-gel ratio, the easier the fibers pulled out, which significantly increased energy consumption and deformation capacity [36]. In addition, the tensile strength of the fiber, the bond between the fiber and the matrix, and the strength of the matrix should also have a certain corresponding relationship to prevent the fiber from breaking, to ensure the pull-out failure of the fiber at the cross-section, and to enhance the tensile strain hardening effect of the material, as well as the multi-crack development characteristics.

**Table 3.** Test results and flexural toughness indexes of specimens.

Specimen	$f_{max}$ (MPa)	$\delta$ (mm)	$\delta_{cr}$ (mm)	$f_{0.35}$ (MPa)	$f_1$ (MPa)	$R_1$	$f_{0.85}$ (MPa)	$R_{0.85}$	$f_{0.2}$ (MPa)	$R_{0.2}$
HC56-0-29	4.62	0.05	0.05	1.25	2.27	1.82	—	—	—	—
HC56-1-29	8.88	0.64	0.09	1.61	6.15	3.82	6.40	3.98	5.45	3.39
HC56-1.5-29	11.49	0.95	0.06	2.00	8.60	4.29	8.81	4.39	7.90	3.94
HC56-2-29	15.32	1.18	0.08	2.67	11.56	4.33	11.80	4.42	9.76	3.65
HC56-2-26	15.04	1.28	0.08	2.45	11.94	4.87	12.03	4.91	11.04	4.51
HC56-2-32	13.32	1.29	0.08	2.05	10.63	5.18	10.86	5.29	9.09	4.43
HC28-1-29	7.33	0.55	0.06	1.27	5.27	4.16	5.58	4.40	5.08	4.01
HC28-1.5-29	11.67	1.09	0.10	2.31	8.25	3.57	8.46	3.66	7.08	3.07
HC28-2-29	15.14	1.85	0.12	2.88	11.72	4.07	11.87	4.13	11.35	3.95
HC28-2-24	15.55	0.87	0.08	2.23	11.14	4.99	11.51	5.16	—	—
HC28-2-26	15.80	1.17	0.08	3.06	11.61	3.79	12.15	3.97	11.52	3.76

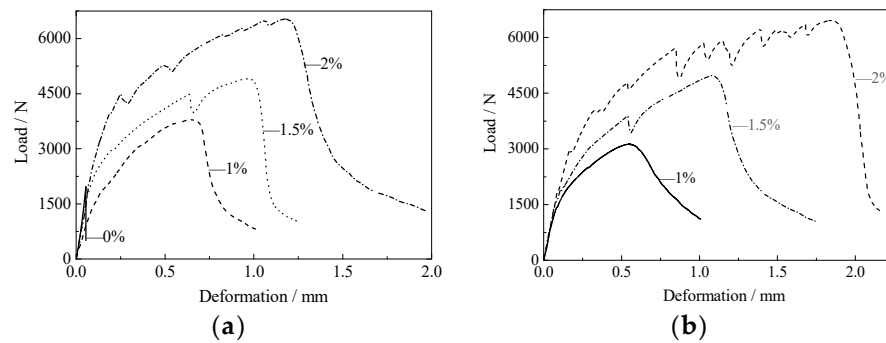


**Figure 7.** Effect of fiber content on load-deflection curves: (a) 56 d; (b) 28 d.

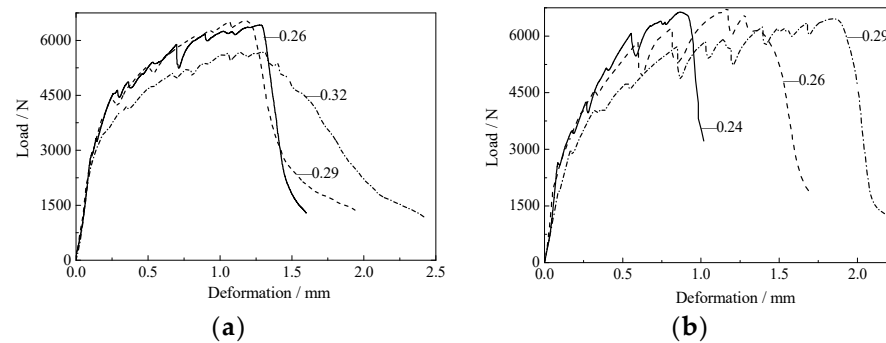


**Figure 8.** Effect of the water-binder ratio of HDC on load-deflection curves: (a) 56 d; (b) 28 d.

As can be seen from Figures 7 and 8, when the age was 28 d, the shape of the load-deflection curve of the HDC specimens and the influence of the different parameters on it were basically the same as those of the 56 d specimens, indicating that 28 d could be used as a measure of standard age for the bending performance of HDC specimens.

#### 4. Methods of Evaluating Bending Toughness of High-Ductility Concrete

##### 4.1. Methods of Evaluating Bending Toughness

The American ASTM C-1018 standard [39] evaluation method is based on the entire process of stress, as shown in Figure 9a, using the mid-span deflection  $\delta$ , toughness index  $I$ , and residual strength index  $R$  of the test specimen when the first crack appears to evaluate the toughness of fiber-reinforced concrete; this is suitable for concrete with a large fiber content and a stable load-deflection curve after cracking. However, all calculations depend on the existence of a large subjective initial crack deflection  $\delta$  and the initial defects of the test piece, which have a great impact on the production of an accurate solution as well as calculation errors. The Japanese Civil Society Standard [40] (JSCE-SF4) defines a toughness factor to characterize the toughness of fiber-reinforced concrete materials, which is the average bending strength when the deflection  $\delta$  of the beam span reaches 1/150, as shown in Figure 9b. The method of evaluating the flexural toughness of fiber-reinforced concrete

in the Chinese CECS 13:2009 standard [41] was improved on this basis. These methods can avoid errors when determining the first crack and evaluating the toughness of concrete with different fiber contents.

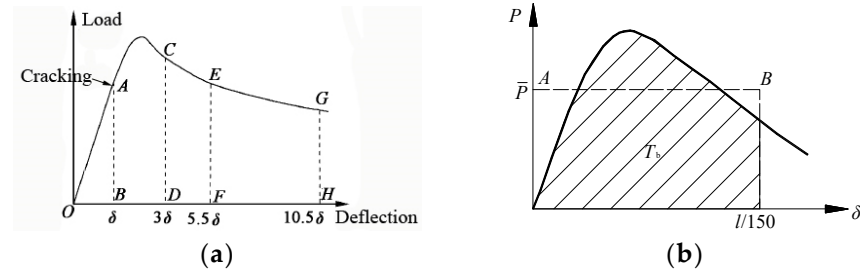


Figure 9. Existing flexural toughness evaluation methods: (a) ASTMC-1018; (b) JSCE-SF4.

It can be seen from Figure 10a that HDC had good deformation capacity. It might still be in the rising section of the load-deflection curve at the specified mid-span deflection. At this time, the material still had a large load-bearing and deformation capacity as well as traditional bending. The toughness evaluation method could not effectively evaluate the bending toughness of HDC. In addition, as shown in Figure 10b, at the same deflection limit, the different specimens might have been in different stress stages, and a bending toughness index calculated using the same deflection limit was not comparable. Therefore, there is an urgent need for a bending toughness evaluation method that can fully reflect the properties of HDC materials, including the aspects of strength and energy, and that can reasonably and accurately evaluate strengthening and toughening effects to control structural strength and ductility from a materials perspective.

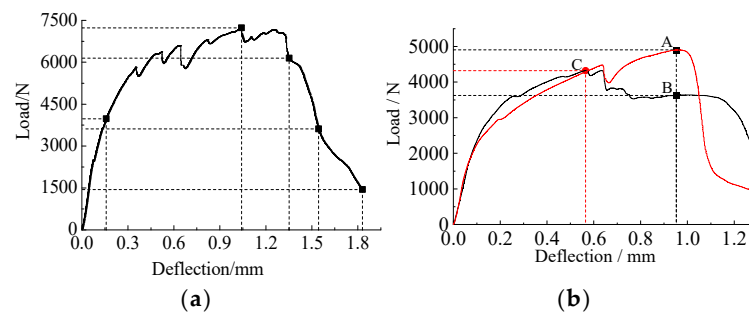


Figure 10. Typical load-deflection curves of HDC: (a) HC56-2-29; (b) HC56-1.5-29.

#### 4.2. Method of Evaluating Bending Toughness Based on Peak Load

With reference to the existing evaluation methods at home and abroad, based on the results of the four-point bending test, we proposed an evaluation method of bending toughness based on the peak load. We used the equivalent bending strength  $f_n$  and bending toughness ratio  $R_e$  to evaluate the bending of HDC from the perspective of strength and energy toughness, as shown in Figure 11.

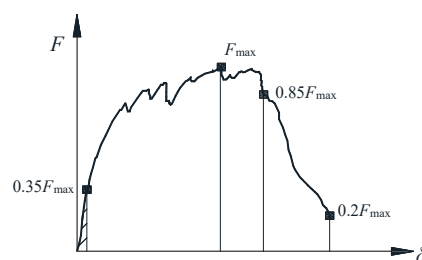


Figure 11. Flexural toughness evaluation method based on peak load.



#### 4.2.1. Equivalent Bending Strength, $f_n$

According to material mechanics, the bending normal stress at the midpoint of the lower edge of a simply supported beam  $f = FL/bh^2$ . When the mid-span deflection is  $\delta$ , the energy is the area under the deflection curve:

$$\Omega = \int_0^{\delta} F(\delta) d\delta = \bar{F}\delta$$

and the equivalent bending strength is:

$$f_n = \frac{\Omega_n L}{bh^2 \delta_n}$$

where  $\Omega_n$  is the area under the load-deflection curve of the bending specimen when the mid-span deflection is  $\delta_n$  (mm);  $\delta_n$  is the corresponding mid-span deflection value (mm) at  $nF_{\max}$ ;  $F_{\max}$  is the peak load of the bending specimen;  $L$  is the support span between the seats (mm); and  $b$  and  $h$  are the cross-section width (mm) and height (mm) of the test piece, respectively. In the rising section of the specimen load-deflection curve,  $n = 0.35$  reflected the strength and toughness of the specimen at the initial crack; in the falling section of the specimen load-deflection curve,  $n = 1, 0.85, 0.50$ , and  $0.20$ , which reflected the peak, the limit, the post-peak strength, and the toughness of the test piece, respectively, and could be used to analyze the ductility, energy consumption, and remaining bearing capacity of the design for continuous collapse resistance.

#### 4.2.2. Bending Toughness Ratio, $R_n$

In order to reflect the toughening effect of the fibers in HDC, the bending toughness ratio  $R_n = f_n/f_{0.35}$  was defined to reflect the fiber bridging effect after the cracking of the specimen as well as the good tensile properties of HDC to improve the bending properties of the material.

Compared with the methods discussed above, this method began from the peak point and used the average stress obtained from the  $0.35 F_{\max}$  front load-deflection curve to characterize the initial cracking performance of the material, which not only effectively improved the stability of the evaluation results but also reduced the dependence on the initial cracking point. In addition, it solved the problem of an insufficient deflection limitation and was suitable for different types of fiber concrete.

The feature points selected in this method were uniformly distributed throughout the loading process, and the bending toughness index could reflect the changing trend in the load-deflection curve, which could comprehensively and accurately evaluate the bending performance of the materials. The larger the peak bending toughness ratio  $R_1$ , the fuller the rising section of the load-deflection curve, the more obvious the pseudo-strain hardening effect of the material, and the larger the toughness index of the falling section, indicating the decline in the load-deflection curve. In actual engineering, several characteristic points can be selected to evaluate the bending toughness of the material as required.

According to the test results, the equivalent bending strength  $f_n$  and bending toughness ratio  $R_n$  of each group of test pieces were calculated by the above method, and  $n = 0.35, 1, 0.85$ , and  $0.20$  were selected. Among them,  $f_1$  and  $R_1$  reflected the reinforcing and toughening effects, respectively, of the fibers in the specimen after cracking and before the peak load. The equivalent bending strengths and bending toughness ratios  $f_{0.85}$ ,  $R_{0.85}$ , and  $f_{0.2}$ ,  $R_{0.2}$  mainly reflected the post-peak performance of the fibers on the specimen.

In this test, due to construction reasons, the test value of the initial cracking strength of the HC28-1-29 group specimens was low, resulting in a higher bending toughness ratio.

#### 4.3. Discussion for Practical Implementation

To prove the effectiveness of the evaluation method of bending toughness based on the peak load, the method was used to measure the flexural toughness of HDC, which produced a strain-hardening effect. These results are useful for practical applications.

As shown in Figure 12, the equivalent bending strength  $f_n$  of HDC significantly increased with the increase in fiber content, but the increase gradually reduced. When the fiber content increased from 0% to 2%, the initial crack equivalent bending strength  $f_{0.35}$  of high-ductility concrete increased by 29%, 25%, and 33%; and the peak equivalent bending strength  $f_1$  increased by 170% and 40%, respectively. The equivalent bending strength  $f_{0.85}$  increased by 182%, 38%, and 34%, and the equivalent bending strength  $f_{0.2}$  after the peak increased by 140%, 45%, and 24%, respectively. This was because the initial cracking performance of the HDC mainly depended on the strength and deformation capacity of the material matrix, so the increase in the amount of fiber to the initial bending equivalent bending strength  $f_{0.35}$  was smaller than that of other stages. In addition, the effects of the water–binder ratio and age on the equivalent bending strength of HDC were relatively small, and the range of change was between 2% and 13%.

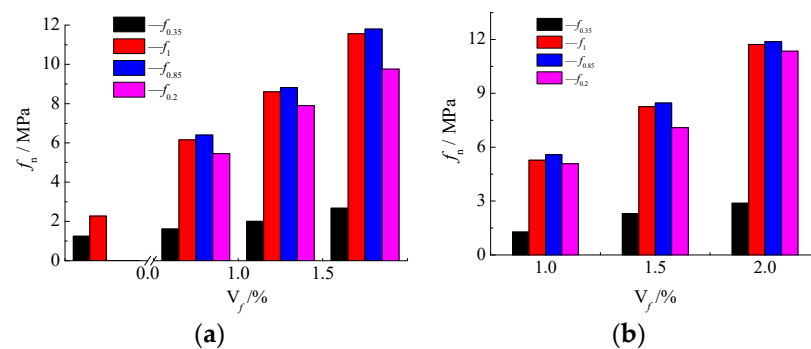


Figure 12. Effect of fiber content on  $f_n$ : (a) 56 d; (b) 28 d.

It can be seen from Table 3 that, compared with the bending toughness ratio of plain concrete, the increase in the bending toughness ratios of the HDC beams  $R_1$ ,  $R_{0.85}$ , and  $R_{0.2}$  reached 184%, 190%, and 143% at the maximum, respectively, indicating that HDC exhibited good cracking performance. A good pseudo-strain hardening effect was achieved and the toughness of plain concrete was significantly improved. This was due to the incorporation of fibers, which made the test piece crack. The fibers at the cracks continued to participate in the force until the fibers were completely pulled out or disconnected. In the process, the energy consumption continued to increase, and the deflection continued to increase. The bending toughness of HDC was significantly better than that of plain concrete.

It can be seen from Figure 13 that the bending toughness ratio  $R_n$  of HDC had an increasing trend with an increase in the fiber content, but the increase gradually decreased, especially when the fiber content increased from 1.5% to 2%. The bending toughness ratio was basically unchanged. The main reason was that the greater the amount of fiber, the easier it was to obtain the strain hardening effect and the development of multiple cracks. The stronger the energy consumption capacity, the better the bending toughness of the material. However, when the fiber content reached a certain value, the effect of further increasing its value on the toughness of the material was not obvious. In addition, as seen in Figures 12 and 13, among the bending toughness indicators of HDC,  $f_{0.85}$  and  $R_{0.85}$  were the largest, indicating that the HDC specimen continued to show a good holding load after the peak load of  $0.85 F_{max}$ , and the load–deflection curve slowly decreased.

Above all, it could be seen that the evaluated results were in good agreement with the experimental specimens, and the novel toughness evaluation method overcame the drawbacks of traditional methods such as an over-dependence on the unstable first cracking characteristics and the uncertain deformability of ductile materials. In addition, the peak load was unique and stable, which provided a determinate foundation of toughness

for evaluating ductile cementitious composites, especially for fiber-reinforced concrete. Therefore, the toughness evaluation based on the peak load is of great help when assessing the performance of novel ductile materials.

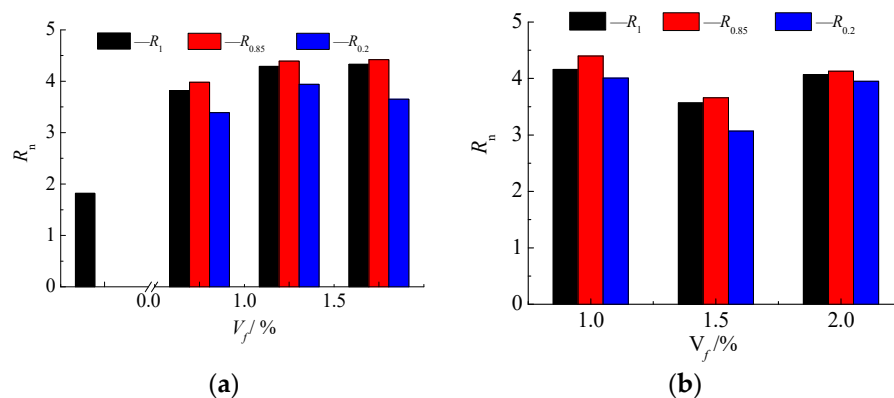


**Figure 13.** Effect of fiber content on  $R_n$ : (a) 56 d; (b) 28 d.

## 5. Conclusions

Based on the results obtained in this research, the following conclusions could be drawn:

- (1) The results indicated that the flexural failure modes, ultimate strength, and toughness of HDC could be improved with an increase in PVA fiber content, especially for deformation. The ultimate flexural strength of HDC with 2% PVA fibers of about 15.32 MPa showed an increase of up to 221%. The deformation and flexural toughness ratios were 23 times and 1.43 times higher than the specimens without fibers, respectively.
- (2) The post-cracking ductility of conventional concrete was significantly improved due to the stress redistribution effect of the fibers. With an increase in PVA fibers, the HDC specimens exhibited better deflection-hardening behavior, characterized by multiple cracks and crack width gradually decreasing. However, the water-binder ratio and age had little influence on the flexural behavior of HDC, with a variation range between 2% and 13%.
- (3) Existing approaches failed to evaluate the flexural toughness of HDC because of their dependence on an unstable initial cracking performance, insufficient deflection limit, and difficulty in reflecting the properties of different tests corresponding with different force stages. Based on JSCE-SF4 and CECS 13: 2009, the equivalent flexural strength and flexural toughness ratios calculated by the peak load of the specimen were proposed to assess HDC flexural toughness, providing a more comprehensive and accurate evaluation by selecting characteristic points evenly distributed throughout the loading process.
- (4) Future recommendations are that the parameter  $n$  of bending toughness based on the peak load should be modified with more data, and the applicability should be proven with more ductile materials.

**Author Contributions:** Conceptualization, Y.D.; Data Curation, Y.L.; Formal Analysis, Y.L.; Funding Acquisition, Y.D.; Investigation, Y.L.; Methodology, Y.L. and J.D.; Project Administration, Y.L. and X.Z.; Supervision, Y.D.; Writing—Original Draft, Y.L. and X.Z.; Writing—Review and Editing, Y.L. and H.X. All authors have read and agreed to the published version of the manuscript.

**Funding:** This work was financially supported by the Henan Key Laboratory of Grain and Oil Storage Facility & Safety (2020KFB04), and the application research plan of key scientific research projects for universities in Henan Province (21A560006).

**Institutional Review Board Statement:** Not applicable.

**Informed Consent Statement:** Not applicable.

**Data Availability Statement:** The corresponding author will provide the datasets created and analyzed during this study upon reasonable request.

**Conflicts of Interest:** The authors declare that they have no conflicting financial interests or personal relationships that may have influenced the work presented in this study.

## Abbreviations

HDC	High-ductility fiber-reinforced concrete
PVA	Polyvinyl alcohol
FRC	Fiber-reinforced concrete
ECC	Engineered cementitious composite
HPFRCC	High-performance fiber-reinforced cementitious composite
SHCC	Strain hardening cementitious composite
d	day
$f_n$	Equivalent bending strength
$R_n$	Bending toughness ratio

## References

- Sukontasukkul, P.; Pomchiengpin, W.; Songpiriyakij, S. Post-crack (or post-peak) flexural response and toughness of fiber reinforced concrete after exposure to high temperature. *Constr. Build. Mater.* **2010**, *24*, 1967–1974. [\[CrossRef\]](#)
- Liu, F.; Ding, W.; Qiao, Y. Experimental investigation on the flexural behavior of hybrid steel-PVA fiber reinforced concrete containing fly ash and slag powder. *Constr. Build. Mater.* **2019**, *228*, 116706. [\[CrossRef\]](#)
- Wu, Z.; Lian, H. *High Performance Concrete*; China Railway Publishing House: Beijing, China, 1999; pp. 1–17. (In Chinese)
- Deng, Z. *The High Performance Synthesis Fiber Reinforced Concrete*; Science Press: Beijing, China, 2003; pp. 45–48. (In Chinese)
- Rashiddadash, P.; Ramezaniapour, A.A.; Mahdikhani, M. Experimental investigation on flexural toughness of hybrid fiber reinforced concrete (HFRC) containing metakaolin and pumice. *Constr. Build. Mater.* **2014**, *51*, 313–320. [\[CrossRef\]](#)
- Stoll, F.; Saliba, J.E.; Casper, L.E. Experimental study of CFRP-prestressed high-strength concrete bridge beams. *Compos. Struct.* **2000**, *49*, 191–200. [\[CrossRef\]](#)
- Cao, M.; Khan, M. Effectiveness of multiscale hybrid fiber reinforced cementitious composites under single degree of freedom hydraulic shaking table. *Struct. Concr.* **2020**, *22*, 535–549. [\[CrossRef\]](#)
- Cao, M.; Xie, C.; Li, L.; Khan, M. Effect of different PVA and steel fiber length and content on mechanical properties of CaCO<sub>3</sub> whisker reinforced cementitious composites. *Mater. Constr.* **2019**, *69*, 200. [\[CrossRef\]](#)
- Kim, H.S.; Shin, Y.S. Flexural behavior of reinforced concrete (RC) beams retrofitted with hybrid fiber reinforced polymers (FRPs) under sustaining loads. *Compos. Struct.* **2011**, *93*, 802–811. [\[CrossRef\]](#)
- Gong, C.; Ding, W.; Mosalam, K.M.; Günay, S.; Soga, K. Comparison of the structural behavior of reinforced concrete and steel fiber reinforced concrete tunnel segmental joints. *Tunn. Undergr. Space Technol.* **2017**, *68*, 38–57. [\[CrossRef\]](#)
- Hou, L.J.; Xu, S.; Zhang, X.F.; Chen, D. Shear Behaviors of Reinforced Ultrahigh Toughness Cementitious Composite Slender Beams with Stirrups. *J. Mater. Civ. Eng.* **2014**, *26*, 467–475. [\[CrossRef\]](#)
- Uygunoğlu, T. Investigation of microstructure and flexural behavior of steel-fiber reinforced concrete. *Mater. Struct.* **2008**, *41*, 1441–1449. [\[CrossRef\]](#)
- Gao, D.; Zhao, L.; Feng, H.; Zhao, S.B. Flexural toughness and its evaluation method of steel fiber reinforced concrete. *J. Build. Mater.* **2014**, *17*, 783–789.
- Felekoğlu, B.; Tosun, K.; Baradan, B. Effects of fibre type and matrix structure on the mechanical performance of self-compacting micro-concrete composites. *Cem. Concr. Res.* **2009**, *39*, 1023–1032. [\[CrossRef\]](#)
- Lin, C.; Kayali, O.; Morozov, E.V.; Sharp, D.J. Influence of fibre type on flexural behaviour of self-compacting fibre reinforced cementitious composites. *Cem. Concr. Compos.* **2014**, *51*, 27–37. [\[CrossRef\]](#)
- Ding, Y.; Zeng, W.; Wang, Q.; Zhang, Y. Topographical analysis of fractured surface roughness of macro fiber reinforced concrete and its correlation with flexural toughness. *Constr. Build. Mater.* **2020**, *235*, 117466.
- Pujadas, P.; Blanco, A.; Cavalaro, S.; Aguado, A. Plastic fibres as the only reinforcement for flat suspended slabs: Experimental investigation and numerical simulation. *Constr. Build. Mater.* **2014**, *57*, 92–104. [\[CrossRef\]](#)
- Blanco, A.; Pujadas, P.; de la Fuente, A.; Cavalaro, S.; Aguado, A. Influence of the type of fiber on the structural response and design of FRC slabs. *J. Struct. Eng.* **2016**, *142*, 04016054. [\[CrossRef\]](#)
- López, J.Á.; Serna, P.; Navarro-Gregori, J.; Camacho, E. An inverse analysis method based on deflection to curvature transformation to determine the tensile properties of UHPFRC. *Mater. Struct.* **2015**, *48*, 3703–3718.
- López, J.Á.; Serna, P.; Navarro-Gregori, J.; Coll, H. A simplified five-point inverse analysis method to determine the tensile properties of UHPFRC from unnotched four-point bending tests. *Compos. Part B Eng.* **2016**, *91*, 189–204. [\[CrossRef\]](#)
- Li, A.; Guo, S.; Zhu, D. Correlation of tensile and flexural behaviors of high toughness cementitious composites. *China Civ. Eng. J.* **2021**, *54*, 54–61.

22. Li, V.C. On engineered cementitious composites (ECC)-a review of the material and its applications. *J. Adv. Concr. Technol.* **2003**, *1*, 215–230. [[CrossRef](#)]
23. Kanda, T.; Li, V.C. Practical Design Criteria for Saturated Pseudo Strain Hardening Behavior in ECC. *J. Adv. Concr. Technol.* **2006**, *4*, 59–72. [[CrossRef](#)]
24. Li, V.C.; Wang, S.; Wu, C. Tensile strain-hardening behavior of polyvinyl alcohol engineered cementitious composite (PVA-ECC). *ACI Mater. J.* **2001**, *98*, 483–492.
25. Naaman, A.E. *High-Performance Construction Materials: Science and Applications*; World Scientific Publishing: Singapore, 2008; pp. 91–153.
26. Parramontesinos, G.J. High-performance fiber-reinforced cement composites: An alternative for seismic design of structures. *ACI Struct. J.* **2005**, *102*, 668–675.
27. Kobayashi, K.; Ahn, D.L.; Rokugo, K. Effects of crack properties and water-cement ratio on the chloride proofing performance of cracked SHCC suffering from chloride attack. *Cem. Concr. Compos.* **2016**, *69*, 18–27. [[CrossRef](#)]
28. Curosu, I.; Mechtcherine, V.; Forni, D.; Cadoni, E. Performance of various strain-hardening cement-based composites (SHCC) subject to uniaxial impact tensile loading. *Cem. Concr. Res.* **2017**, *102*, 16–28. [[CrossRef](#)]
29. Deng, M.; Han, J. Analysis of compressive toughness and deformability of high ductile fiber reinforced concrete. *Adv. Mater. Sci. Eng.* **2015**, *3*, 384902. [[CrossRef](#)]
30. Dang, Z.; Liang, X. Cyclic behavior of shear walls with HPFRCCs in the inelastic deformation critical region. *Struct. Des. Tall Spec.* **2016**, *25*, 886–903. [[CrossRef](#)]
31. Deng, M.; Dai, J.; Lu, H.; Liang, X. Shear capacity and failure behavior of steel-reinforced high ductile concrete beams. *Adv. Mater. Sci. Eng.* **2015**, *2015*, 845490. [[CrossRef](#)]
32. Deng, M.; Ma, F.; Ye, W.; Liang, X. Investigation of the shear strength of HDC deep beams based on a modified direct strut-and-tie model. *Constr. Build. Mater.* **2018**, *172*, 340–348. [[CrossRef](#)]
33. Dong, L.H.; Xu, S.L. Research on flexural properties and flexural toughness evaluation method of ultra high toughness cementitious composites. *China Civ. Eng. J.* **2010**, *43*, 32–39. (In Chinese)
34. Skazlić, M.; Bjegović, D. Toughness testing of ultra high performance fibre reinforced concrete. *Mater. Struct.* **2009**, *42*, 1025–1038. [[CrossRef](#)]
35. Li, J.; Wan, C.; Niu, J.; Wu, L.; Wu, Y. Investigation on flexural toughness evaluation method of steel fiber reinforced lightweight aggregate concrete. *Constr. Build. Mater.* **2017**, *131*, 449–458. [[CrossRef](#)]
36. Deng, Z.C.; Liu, G.P.; Du, C.; Shi, H.C. Flexural toughness and its characterization of a new kind of Macro-polyolefin fiber reinforced concrete plate. *J. Build. Mater.* **2015**, *18*, 7–11. (In Chinese)
37. Zhao, S.; Sun, X.; Li, C. Flexural toughness of steel fiber reinforced high-strength concrete. *J. Build. Mater.* **2003**, *6*, 95–99. (In Chinese)
38. Liu, Z.; Li, Y.; Wen, C. Experimental study on strength and deformation performance of PVA-ECC under splitting tension. *J. Build. Mater.* **2016**, *19*, 746–751. (In Chinese)
39. ASTM C 1018; Standard Test Method for Flexural Toughness and First Crack Strength of Fiber Reinforced Concrete (Using Beam with Third-Point Loading). ASTM International: West Conshohocken, PA, USA, 1997; pp. 544–551.
40. JSCE-SF4; Method of Test for Flexural Strength and Flexural Toughness of Fiber Reinforced Concrete. Japan Concrete Institute: Tokyo, Japan, 1984; pp. 45–51.
41. CECS 13:2009; China Association for Engineering Construction Standardization. Test Method Used for Steel Fiber Reinforced Concrete. China Planning Press: Beijing, China, 2010; pp. 54–59. (In Chinese)